

# SYNERGISTIC RETRIEVALS OF LIQUID WATER CLOUD PROPERTIES FROM SYNTHETIC DATA

Simone Placidi<sup>1</sup>, Rob A. Roebeling<sup>2</sup>, Dave P. Donovan<sup>2</sup>, Herman W.J. Russchenberg<sup>1</sup>

<sup>1</sup>IRCTR – Delft University of Technology, 2600 GA Delft, The Netherlands

<sup>2</sup>KNMI – Royal Netherlands Meteorological Institute, 3730 AE De Bilt, The Netherlands

S.Placidi@tudelft.nl, Rob.Roebeling@knmi.nl

## Abstract

Optical and microphysical properties of liquid water clouds are required for a better understanding of the interactions between aerosols, clouds and radiation in order to describe the first indirect aerosol effect and the solar radiation feedback. The two cloud properties involved in the monitoring of the first indirect aerosols effect are the cloud geometrical thickness and the cloud droplet number concentration. The retrieval of these two cloud properties from satellite observations improves the large scale and simultaneous mapping of the first indirect aerosol effect along with other cloud properties such as liquid water path, effective radius and optical thickness. In this work the synergy of active instruments, cloud radar and lidar, along with satellite observations from passive sensors is applied in order to determine correctly the cloud droplet concentration and cloud depth from simulated data.

The ESA EarthCARE Simulator, ECSIM, is modified and used to generate the dataset for simulated observations of the ground-based cloud radar and lidar as well as the passive satellite reflectances. Afterwards, the KNMI Cloud Physical Properties (CPP) algorithm used to retrieve optical and microphysical cloud properties is applied to the simulated reflectances. These simulated set of measurements are generated for different stratocumulus cloud fields including simple (quasi)-adiabatic plane-parallel clouds and a “realistic” cloud generated from cloud resolving models.

The retrieved cloud properties from the CPP applied to the simulated reflectances are compared simultaneously to the cloud properties of the original scene to observe the deviation of the retrieved properties from the true original cloud properties. This paper wants to show the potentials and the use of ECSIM simulated data for algorithm developments and improvements. The comparisons of the CPP retrieved cloud properties applied to the simulated reflectances with the original values of the cloud scenes show very good agreement and a new consistent way for developing retrieval algorithms.

## INTRODUCTION

One of the major uncertainties with respect to climate forcing is the treatment of water clouds and their interaction with solar and thermal radiations. Modern meteorological and climate models treat clouds in a simple way mainly because of the large variability in relevant cloud properties at small and large scales. Accurate information on cloud properties and their spatial and temporal variations are required. Satellite observations provide useful long-term observations on cloud properties and their spatial and temporal variations on a large scale starting from measuring the radiances of the clouds. Various methods have been developed to retrieve cloud optical and microphysical properties from passive satellite observations, such as cloud particle size ( $R_{eff}$ ), cloud optical thickness ( $COT$ ), cloud liquid water path ( $CLWP$ ), cloud geometrical thickness ( $h$ ) and cloud droplet number concentration ( $N$ ). The accurate retrieval of the latter two cloud properties from geostationary satellite would give the opportunity to accurately describe the first indirect aerosol effect for a large spatial and temporal scale.

Several authors implemented models of vertical distribution of cloud microphysical and optical properties to simulate cloud geometrical thickness and droplet concentration using  $COT$  and  $R_{eff}$  retrieved

from passive imager satellite radiances (Nakajima and King, 1990). Some authors in their models assume water clouds to be simply adiabatic (Breguier et al., 2000; Szczodrak et al., 2001), while others apply a quasi-adiabatic water cloud model taking into consideration the effects of mixing and entrainment (Boers et al., 2006). Apart from those methods, Schuller et al., 2003, retrieves cloud depth and droplet concentration directly from satellite radiances, performing the radiative transfer calculations for clouds using prescribed Look-Up Tables for droplet concentration and liquid water content profiles.

The method by Boers et al, is used in this work to retrieve  $N$  and  $h$  starting from the satellite retrieved  $R_{eff}$  and  $COT$  as input. The comparison of  $h$  with the cloud geometrical thickness observed by active instruments like ground-based radar and lidar, removes one unknown in the model and improve the accuracy of the droplet number concentration retrieval (Roebeling et al, 2008). Sensor synergy between ground-based profiling instruments and satellite passive sensors is needed for more accurate studies of cloud properties. Satellite observations, in fact, complement and extend the ground-based observations by providing increased spatial coverage and different observation methods. In order to exploit possible sensor synergy techniques for ground- and space-based sensors there is the need of co-located measurements in time and space. The lack of simultaneous observational data for liquid water clouds makes the sensor synergy a difficult task for these clouds. Because of the small amount of cases with stratocumulus clouds and data observed by several instruments, a synthetic dataset with several cases is created and used for the analysis of the retrieval algorithm of cloud geometrical thickness and cloud droplet number concentration.

## THE SYNTHETIC DATASET

The synthetic dataset is generated with the EarthCARE simulator - ECSIM (Voors et al, 2007). ECSIM generates ground- and space-based radar and lidar observations as well as the satellite Bidirectional Reflectance Distribution Functions - BRDF at the top of the atmosphere for the same cloud scenario. The KNMI-CPP retrieval algorithm is afterward applied to the simulated BRDFs and the cloud properties are retrieved. ECSIM allows the creation of a complete synthetic set of observations (lidar-radar-radiometer) for several and diverse cloud scenes. In this paper, three different scenes describing stratocumulus clouds are analyzed and their cloud properties retrieved with the KNMI-CPP algorithm and compared with the original cloud scene properties.

### The EarthCARE Simulator - ECSIM

The EarthCARE simulator - ECSIM is a computational tool which can simulate the complete EarthCARE mission. This simulator uses several forward and retrieval models, utility programs and plotting tools to simulate and visualize what the EarthCARE measurements and retrievals would be. ECSIM can simulate all the 4 instruments aboard EarthCARE satellite, such as the 94-GHz cloud profiling radar, the high spectral resolution lidar at 353 nm, the multispectral imager and the broad-band radiometer. Its use is rather straightforward: given a cloud scene as input and chosen the instruments to be simulated, ECSIM runs the selected models and simulations and gives netcdf file outputs for every chosen instrument for further data analysis. The cloud scenes, as input for the simulations, can be created using the embedded ECSIM cloud generator or they can be converted from Cloud Resolving Models or from Large Eddy Simulation models to ECSIM standard input cloud scene.

#### *Ground-based Simulations*

The original ECSIM configuration, space-based oriented, has been upgraded including new models, in order to simulate also ground-based radar and lidar observations. The new models can simulate ground-based lidar and radar measurements for different configurations. In this work, the radar system is a 94 GHz cloud profiling radar with 50 meters vertical resolution, while the lidar emits at 532 nm and collects observations with the same vertical resolution as the radar. The geometry of the cloud scene for the upward-looking configuration sets up the satellite at 1 meter above the ground with a speed in the along-direction of  $10 \text{ m/s}$ , in this way it results like if the cloud moves above the ground-based upward-looking instrument at  $10 \text{ m/s}$  speed.

ECSIM can simulate the seven shortwave channels of the Multi Spectral Imager (0.660, 0.865, 1.61, 2.20, 8.8, 10.8, 12.0 microns) with their BRDFs. The shortwave calculations are computed using the shortwave model which allows to work with two different radiative transfer models. The Shortwave Radiation model can be set to operate with 1-D or 3-D mode. The two radiative transfer models implemented in ECSIM are:

- a 3-D Monte-Carlo solver
- an Independent Column Approximation mode using the DISORT solver.

ECSIM has been also modified in order to simulate the BRDF observed with MODIS and SEVIRI's channels, adding new correlation-k tables for both satellites. These include the MODIS' 0.645, 0.858, 1.24, 1.64, 2.13, and 3.75  $\mu m$  and the SEVIRI's 0.635, 0.81, 1.64, and 3.92  $\mu m$  channels. In this work only the configuration from the EarthCARE original MSI forward model is used along with the independent column approximation solver and an output resolution of 2 Km for the first two scenes and 0.1 Km for the Astex scene. However, ECSIM can run the simulations using the MODIS or SEVIRI configurations and any output resolution value, independently.

The BRDFs, together with the Sun-satellite geometry and other auxiliary data from the simulations, are used as input for the Cloud Physical Properties (CPP) retrieval algorithm (Roebeling et al., 2006). The CPP retrieval algorithm has been developed at the Royal Netherlands Meteorological Institute (KNMI) as part of the EUMETSAT Climate Monitoring Satellite Application Facility. This algorithm retrieves  $COT$  and  $R_{eff}$  in an iterative manner, by comparing satellite observed or simulated reflectances at visible (0.6 $\mu m$ ) and near-infrared (1.6 $\mu m$ ) to the reflectances simulated with the Doubling Adding KNMI - DAK radiative transfer model. The DAK radiative transfer model (De Haan et al. 1987; Stammes 2001) is used to simulate reflectances for plane-parallel clouds embedded in a midlatitude summer atmosphere. The underlying surface is assumed to be Lambertian, for which the reflectances were obtained from MODIS white-sky albedo data. The vertical distribution of the assumed spherical cloud droplets is parameterized in terms of the effective radius, using a modified gamma distribution with an effective variance of 0.15. The cloud reflectances for the Look-Up Tables are simulated at 0.6, 0.8, 1.6, 2.1, 3.8  $\mu m$ , for optical thicknesses between 0 and 256 and droplet effective radii between 1 and 24  $\mu m$ . The  $CLWP$ , assuming a fixed vertical profile for liquid water content, is computed from the  $COT$  and  $R_{eff}$  using the following formula:

$$CLWP = \frac{2}{3} * COT * R_{eff} * \rho \quad (1)$$

Furthermore, the cloud geometrical thickness  $h$  and the cloud droplet number concentration  $N$  are retrieved according to the quasi-adiabatic cloud model described in Boers et al., 2006. This model parameterizes the vertical variation of cloud microphysical and optical properties. The essential point of the cloud model is that  $COT$  and  $R_{eff}$  are explicit functions of  $N$  and  $h$ . The algorithm contains implicit assumptions about the nature of basic thermodynamic and microphysical points that introduce uncertainties in the retrieved properties. However, referring to previous studies (Boers et al., 2006), the sub-adiabatic character of the cloud is the only variable parameter to take into consideration. In the sensitivity studies, it is, indeed, found that the major source of uncertainty in the retrieval is the sub-adiabatic behaviour of the cloud, which is expressed by the sub-adiabatic fraction parameter. Deviations from the adiabatic cloud, (sub-adiabatic fraction parameter equal to 1.0), due to turbulent entrainment and vertical mixing lead to an increase of  $h$  and a decrease of  $N$ . The sub-adiabatic fraction parameter for the retrieval of the first two cloud scenes is set to 0.7, while for the "realistic" Astex scene is set to 0.3, showing the non-adiabatic character of the cloud field. However, more detailed investigations on the Astex scene characteristics have to be made to confirm their non-adiabatic nature.

### Simulated Cloud Scenes

The selected cloud scenes for the simulations refer to three different cloud configurations and scenarios which can be easily used as reference for the radiative transfer models and the satellite retrievals. The three cloud scenes are:

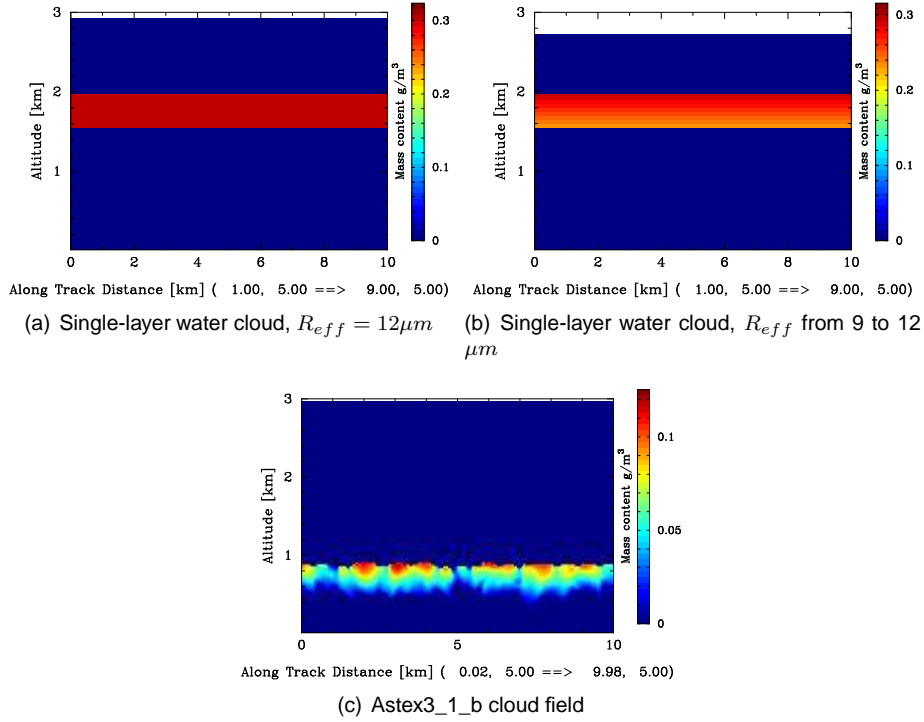


**Figure 1: Mass Content extracted from the original cloud scenes**

1. Plane-parallel single-layer stratocumulus with  $R_{eff}$  constant in height equal to  $12 \mu m$  [fig. 1(a)]
2. Plane-parallel single-layer stratocumulus with  $R_{eff}$  increasing in height from 9 to  $12 \mu m$  [fig. 1(b)]
3. Inhomogenous stratocumulus cloud field from the ASTEX campaign generated by CRM [fig. 1(c)]

Figure 1 plots the mass content of the scenes showing where the hydrometeors are located and how much water is present within the cloud in  $g/m^3$ . Figure 1 is used to describe the original structure of the clouds and as a reference for each scene.

The first two scenes describe a single-layer stratocumulus cloud parallel to the ocean surface with no presence of drizzle. The cloud droplets within their 500 meters thickness are distributed according to a gamma distribution with shape parameter set to 9 and the droplet sizes range from 0 to  $50 \mu m$ . The only difference between scene 1 (fig. 1(a)) and scene 2 (fig. 1(b)) is about the characteristic of their  $R_{eff}$ . In fact, scene 1 present one constant effective radius in height with value of  $12 \mu m$  whilst in scene 2 the  $R_{eff}$  is increasing linearly from  $9 \mu m$  at the cloud base to  $12 \mu m$  at the cloud top.

The third scene can be defined as a "realistic" scene, in fact, it is modelled with Cloud Resolving Model (CRM) simulations after the Astex cloud campaign, (Albrecht et al., 1995). This scene (fig. 1(c)) present inhomogeneity in the vertical and horizontal domain and it has a very high resolution of about 50 meters in both vertical and horizontal dimensions.

## SIMULATION OUTPUTS

After the description of the ECSIM's characteristics and the cloud scenes selected for the simulations, the outputs are described for each of the cloud scene. The first two scenes, being homogeneous in the horizontal domain, are described with the plots of the profiling instruments and only a table for the results retrieved with the KNMI CPP algorithm and compared to the original true values of the cloud scene. The outputs of the third scene are described with the plots from the profiling instruments, the plots of the horizontal cloud properties retrieved from the CPP and with one table listing the statistical analysis of the original and retrieved cloud properties.

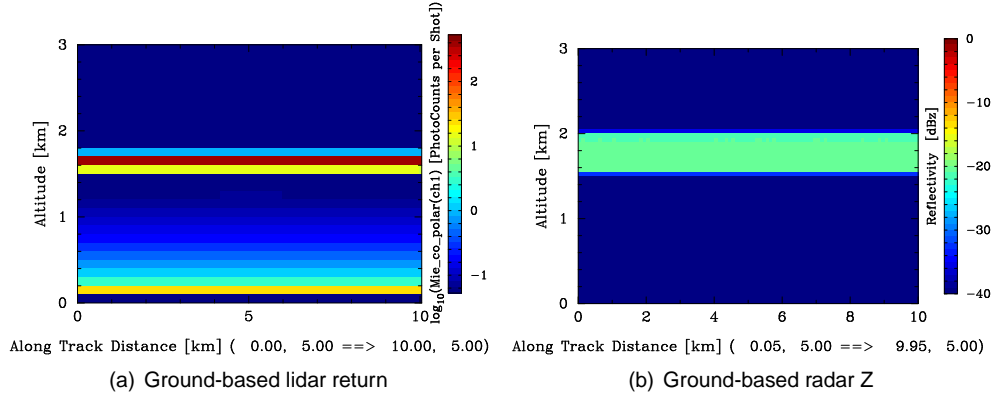


**Figure 2: Ground-based lidar and radar simulation outputs for the single-layer stratocumulus cloud**

### SCENE 1

Figure 2 shows the simulation outputs for the ground-based copolar return lidar signal (fig. 2(a)) and the radar reflectivity (fig. 2(b)). Both the radar and lidar detect the stratocumulus cloud and the synergy of the two instruments results in the retrieval of the cloud geometrical thickness. In table 1 the original properties of the first cloud scene are shown in the first column, while on the second column, the values retrieved after applying the CPP to the ECSIM simulated BRDFs are displayed. It can be noted the very good agreement for all the cloud properties between the original true values and the retrieved ones.

	Scene 1	CPP retrieval
<b>COT</b> [-]	17.8	17.8
<b>REFF</b> [ $\mu$ ]	12	12.07
<b>LWP</b> [ $g/m^2$ ]	136	143.55
<b>h</b> [m]	500	509
<b>N</b> [ $1/cm^{-3}$ ]	58	69

**Table 1:** Comparison of cloud properties for scene 1

	Scene 2	CPP retrieval
<b>COT</b> [-]	17.8	17.5
<b>REFF</b> [ $\mu$ ]	10.5	10.8
<b>LWP</b> [ $g/m^2$ ]	119	125
<b>h</b> [m]	500	495
<b>N</b> [ $1/cm^{-3}$ ]	76	83.5

**Table 2:** Comparison of cloud properties for scene 2

### SCENE 2

Scene 2, described in table 2, presents almost the same cloud properties than cloud scene 1, except in the vertical variation of the  $R_{eff}$  within the cloud. In fact,  $R_{eff}$  increases linearly from 9 microns at the cloud bottom to 12 microns at the cloud top. The original  $COT$  is maintained the same, but  $R_{eff}$  is different. The radar can describe this feature of having a linear vertical variation of the  $R_{eff}$  in the observed radar reflectivity (fig. 3(b)). Table 2 shows the original values of the cloud scene in the column named “Scene 2” while in the “CPP retrieval” column the retrieved values are inserted. It is fairly easy to see the good agreement between the retrieved values and the true cloud properties. The small errors can be attributed to the different ways of calculating the cloud properties.

### SCENE 3

The simulation outputs referring to the “realistic” ASTEX scene are also run with the ICA mode in order to be consistent with the CPP look-up tables. However, they could have been run with the Monte-Carlo mode taking into account the 3-D effects showing up when the cloud field is not homogeneous. The vertical and horizontal cloud distribution can be seen from the ground-based observations in fig. 4. The satellite observations and retrievals are shown in the plots in the right-hand side of figure 5 while the plots on the left-hand side shows the original “true” cloud properties. The upper plots show the optical thickness,  $COT$ , of the original scene (fig. 5(a)) and the one retrieved from the CPP algorithm; the plots in the middle show the liquid water path,  $CLWP$ , while the two bottom plots exhibit the patterns for the cloud droplet number concentration  $N$ . The three retrieved cloud properties show very good, accurate and consistent agreement in describing the pattern of the inhomogeneous cloud field all over

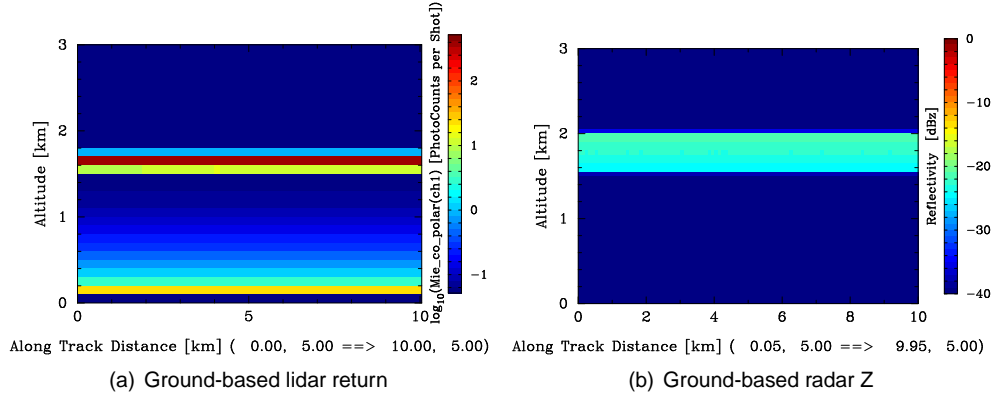


**Figure 3: Ground-based lidar and radar simulation outputs for the single-layer stratocumulus with increasing  $R_{eff}$**

its horizontal 9 Km domain. In table 3 the statistics for the five cloud properties are listed for the original cloud field values ("Scene 3" column) and for the CPP retrieved values ("CPP retrieval" column). Generally, the mean values of the retrieved cloud properties match the mean values of the original cloud scene with very small differences. Even the standard deviations are in good agreement for most of the cloud properties except for the  $R_{eff}$ . The mismatch in the  $R_{eff}$  standard deviation is due to the fact that the Astex scene is generated with almost constant  $R_{eff}$  over the domain with values between 5 and 7  $\mu m$ , while the CPP shows higher values for few points in the domain. Overall, figure 5 and table 3 show that the CPP retrievals are very consistent also to retrieve correct cloud properties for the inhomogeneous cloud field.

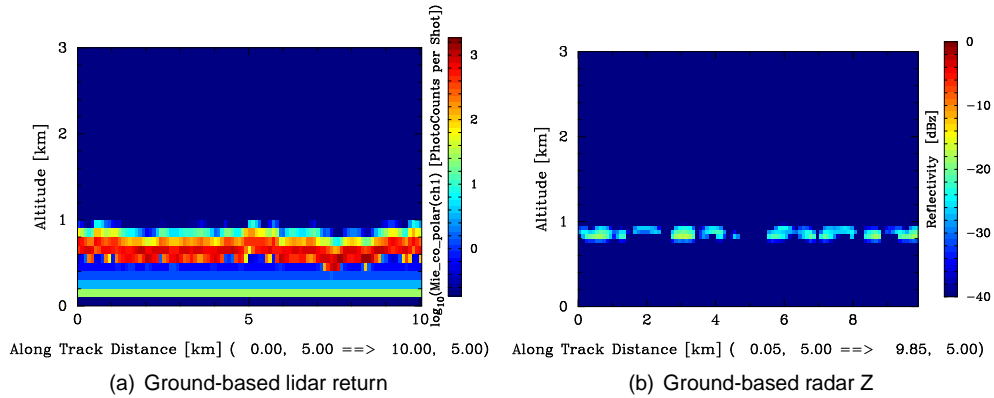


**Figure 4: Ground-based lidar and radar simulation outputs for the ASTEX cloud scene**

## SUMMARY AND FUTURE WORKS

This work shows the use of synthetic data generated from the EarthCARE Simulator - ECSIM for the analysis of satellite retrieval techniques and new sensors synergy algorithm developments. The ECSIM generated cloud scenes are described and simulated for the ground-based radar, lidar and the EarthCARE Multi Spectral Imager in 1-D mode. The output of the simulations for the three instruments and the three scenes makes available a complete synthetic dataset of data for the analysis of the CPP retrieval.

The KNMI-CPP retrieves cloud properties that show very high agreement with the true values of the original scenes. The importance of using ECSIM to create simple plane-parallel single-layer clouds with personalized cloud properties helps in studying the sensitivity, accuracy of the retrieval algorithms or for improving them. According to the simulation outputs and the original values of the clouds, the cloud droplet number concentration and the geometrical thickness retrieval model is working fine as

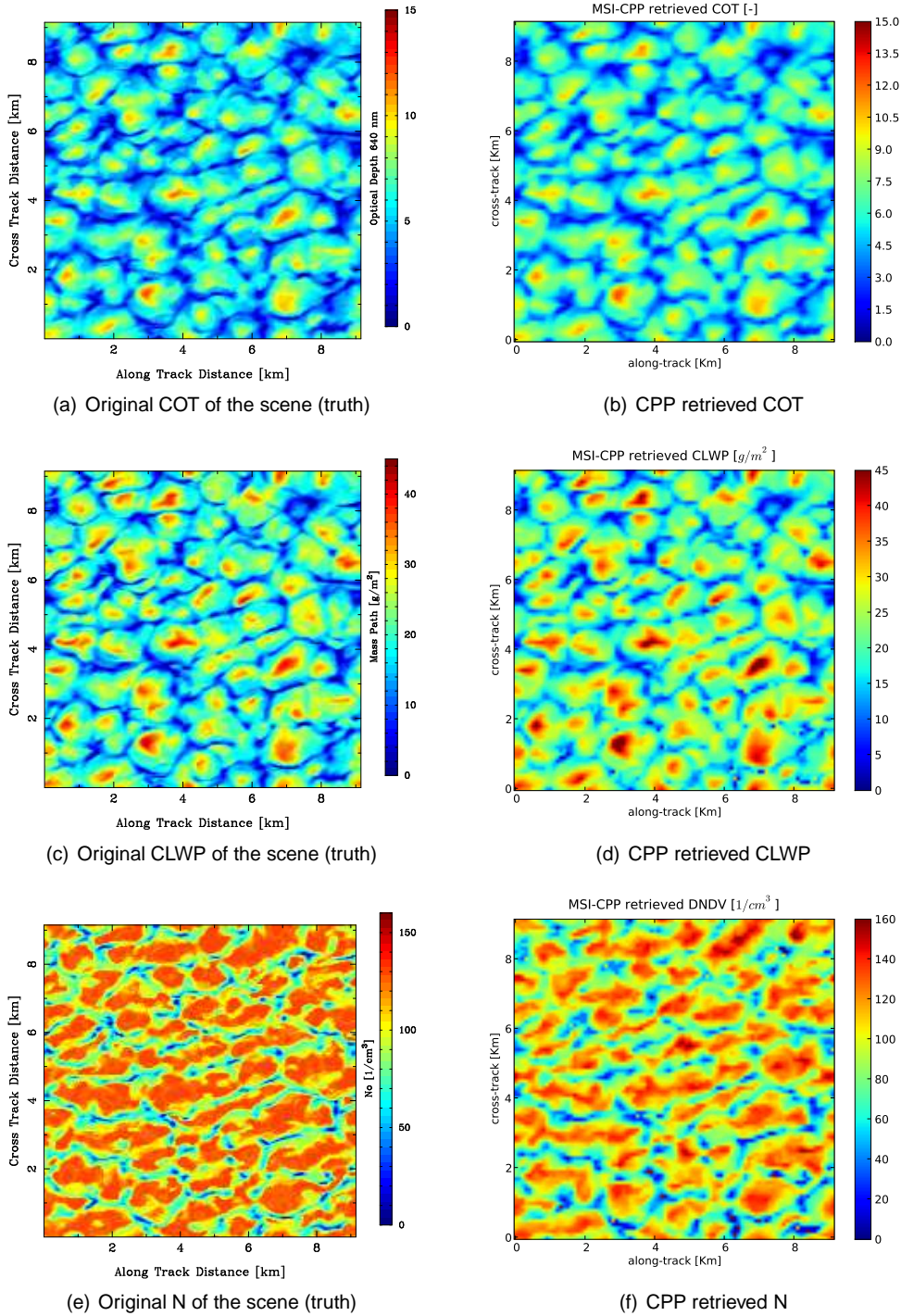


**Figure 5: Comparison of the original cloud properties with the ones retrieved by the CPP algorithm**

long as the cloud sub-adiabatic fraction is correctly set for the cloud cases.

New methods to make the cloud sub-adiabatic factor dynamic and adaptive to different cloud situations should be investigated in the future in order to have a better monitor of the aerosols indirect effects. Future work will also focus on the simulations of the shortwave model with the 3-D Monte-Carlo mode for the Astex scene in order to quantify the range of 3-D effects with respect to the satellite retrievals.

		Scene 3	CPP
<b>COT</b> [–]	mean	5.73	5.82
	std	2.07	2.01
<b>REFF</b> [ $\mu$ ]	mean	5.71	5.59
	std	0.36	0.78
<b>LWP</b> [ $g/m^2$ ]	mean	20.14	21.58
	std	7.09	7.46
<b>h</b> [m]	mean	380.81	384.36
	std	83.6	65.21
<b>N</b> [ $1/cm^3$ ]	mean	96.96	96.72
	std	34.88	35.83

**Table 3:** Comparison of cloud properties for scene 3

## ACKNOWLEDGEMENTS

We acknowledge the Université du Québec à Montréal (UQAM) for providing the ASTEX cloud scene used in this work.

## REFERENCES

- Albrecht, B. A., C.S.Bretherton, D.W.Johnson, W.H.Schubert and A.Shelby Frisch, 1995: The Atlantic Stratocumulus Transition Experiment – ASTEX. *Bull. Amer. Meteor. Soc.*, **76**, 889-904.
- Boers, R., J. R. Acarreta, and J. L. Gras (2006), Satellite Monitoring of the First Indirect Aerosol Effect: Retrieval of Cloud Droplet Concentration, *J. Geophys. Res.*, **111**
- De Haan, J. F., P. Bosma, and J. W. Hovenier (1987), The adding method for multiple scattering calculations of polarized light, *J. Astron. Astrophys.*, **183**, 371-391.
- Donovan D.P., Voors, R.H., van Zadelhoff, G.-J. and Acarreta, J.R., 2008: ECSIM Models and Algorithms Document
- Nakajima, T. and M.D.King (1990), Determination of the optical thickness and effective particle radius of clouds from reflected solar radiation measurements.part I.Theory, *J.Atmos.Sci.*,**47**, 1878-1893
- Roebeling, R.A., A.J. Feijt, and P. Stammes (2006), Cloud property retrievals for climate monitoring: implications of differences between SEVIRI on METEOSAT-8 and AVHRR on NOAA-17, *J. Geophys. Res.*, **11**
- Roebeling, R.A., H.M. Deneke and A.J. Feijt, (2008) Validation of cloud liquid water path retrievals from SEVIRI using one year of CLOUDNET observations, *J. Appl. Meteor.*, **47**, 206-222.
- Roebeling, R.A., S. Placidi, D.P.Donovan, H.W.J.Russchenberg and A.J.Feijt, (2008), Validation of liquid property retrievals from SEVIRI using ground-based observations, *Geophys. Res. Lett.*, **35**
- Schüller, L., J. L. Brenguier, and H. Pawlowska (2003), Retrieval of microphysical, geometrical, and radiative properties of marine stratocumulus from remote sensing, *J. Geophys. Res.*, **108**, 8631
- Szczodrak, M., P.H. Austin, and P. Krummel (2001), Variability of optical depth and effective radius in marine stratocumulus clouds. *J. Atmos. Sci.*, **58**, 2912-2926
- Stammes, P. (2001), Spectral radiance modeling in the UV-Visible range.IRS 2000: Current problems in Atmospheric Radiation, edited by W.L.Smith and Y.M. Timofeyev, 385-388, A. Deepak Publ., Hampton, Va.
- Voors, R., Donovan D.P., Acarreta J.R., Eisinger M., Franco R., Lajas D., Moyano R., Pirondini F., Ramos J., and Wehr T., 2007: ECSIM: the simulator framework for EarthCARE, *Proc. SPIE* 6744